

Higgs-photon production at $\mu\bar{\mu}$ colliders

Ali Abbasabadi¹, David Bowser-Chao², Duane A. Dicus³ and Wayne W. Repko⁴

¹*Department of Physical Sciences, Ferris State University, Big Rapids, Michigan 49307*

²*Department of Physics, University of Illinois at Chicago, Chicago, Illinois 60607*

³*Center for Particle Physics and Department of Physics*

University of Texas, Austin, Texas 78712

⁴*Department of Physics and Astronomy*

Michigan State University, East Lansing, Michigan 48824

(May 13, 2019)

Abstract

We present cross sections for the reaction $\mu\bar{\mu} \rightarrow H\gamma$ over a range of $\mu\bar{\mu}$ collider energies. The amplitudes for this process receive tree level contributions and one-loop contributions, which are of comparable magnitude. The tree level amplitudes are dominated by helicity non-flip terms and the one-loop amplitudes are dominated by helicity flip terms. As a consequence, the interference terms between the tree level and one-loop contributions are negligible. For a 500 GeV $\mu\bar{\mu}$ collider, the cross section for $H\gamma$ associated production approaches 0.1 fb.

14.80.Bn, 13.10.+q

I. INTRODUCTION

Recently, the possibility of using $\mu\bar{\mu}$ colliders to investigate the properties of Higgs-bosons has received considerable attention [1,2]. There are significant advantages to studying Higgs-bosons with this type of collider, particularly if the mass is known from its discovery at, say, the LHC or NLC [2]. Under these circumstances, the width and branching ratios can be studied at the Higgs pole.

In the report, we present results for the cross section $\mu\bar{\mu} \rightarrow H\gamma$ and discuss its use in determining properties of the Standard Model Higgs-boson. At a muon collider, unlike an electron-positron collider, the Higgs-boson-muon coupling is sufficiently large to make the tree level amplitude for $H\gamma$ associated production of comparable size to the one-loop amplitude [3]. The contribution of the latter, not included in Ref. [3], is given here together with a discussion of the helicity dependence of both the one-loop and tree level amplitudes.

The tree level amplitudes are given in the next section. Section III contains a summary of the one-loop amplitudes, and this is followed by a discussion.

II. TREE LEVEL AMPLITUDES

The tree level diagrams for $\mu\bar{\mu} \rightarrow H\gamma$ are shown in Fig. 1, and the resulting amplitude is

$$\mathcal{M}^{\text{tree}} = \frac{egm_\mu}{2m_W} \left[-i \left(\frac{p \cdot \epsilon^*}{p \cdot k} - \frac{\bar{p} \cdot \epsilon^*}{\bar{p} \cdot k} \right) \bar{v}(\bar{p})u(p) + \left(\frac{1}{2p \cdot k} + \frac{1}{2\bar{p} \cdot k} \right) \bar{v}(\bar{p})\sigma_{\mu\nu}k_\nu u(p) \epsilon_\mu^* \right], \quad (1)$$

where p is the momentum of the μ , \bar{p} the momentum of the $\bar{\mu}$, k the momentum of the γ and ϵ its polarization. For massless muons, only the helicity non-flip contributions from the factors $\bar{v}(\bar{p})u(p)$ and $\bar{v}(\bar{p})\sigma_{\mu\nu}u(p)$ are non-zero. Thus, we expect the helicity flip tree amplitudes to contain a factor of order m_μ/E relative to the non-flip amplitudes. Explicitly, we find,

$$\mathcal{M}_{\lambda\bar{\lambda}\lambda_\gamma}^{\text{tree}} = -i \frac{egm_\mu}{\sqrt{2}m_W} \left(\frac{1}{2p \cdot k} + \frac{1}{2\bar{p} \cdot k} \right) \begin{cases} \sin \theta [\lambda_\gamma(2|\mathbf{p}|^2 - E\omega) + |\mathbf{p}|\omega] & , \lambda\bar{\lambda} = ++ \\ \sin \theta [\lambda_\gamma(2|\mathbf{p}|^2 - E\omega) - |\mathbf{p}|\omega] & , \lambda\bar{\lambda} = -- \\ m_\mu \omega(1 + \lambda_\gamma \cos \theta) & , \lambda\bar{\lambda} = +- \\ m_\mu \omega(1 - \lambda_\gamma \cos \theta) & , \lambda\bar{\lambda} = -+ \end{cases}, \quad (2)$$

where E is the muon energy in the center of mass, $|\mathbf{p}| = \sqrt{E^2 - m_\mu^2}$, ω is the photon energy, θ is the photon scattering angle and $\lambda_\gamma = \pm 1$ is the photon helicity. It can be seen that the helicity flip amplitudes have a factor of m_μ .

III. ONE-LOOP AMPLITUDES

The one-loop amplitudes for $\mu\bar{\mu} \rightarrow H\gamma$ receive contributions from pole diagrams involving virtual photon and Z exchange and from various box diagrams containing muons, gauge bosons and/or Goldstone bosons [4,5]. There are also double pole diagrams whose contribution vanishes. This is illustrated in Fig. 2. In the non-linear gauges we chose [4], the

full amplitude consists of four separately gauge invariant terms: a photon pole, a Z pole, Z boxes and W boxes. These amplitudes can be written as

$$\mathcal{M}_{\text{pole}}^\gamma = \frac{\alpha^2 m_W}{\sin\theta_W} \bar{v}(\bar{p})\gamma_\mu u(p) \left(\frac{\delta_{\mu\nu} k \cdot (p + \bar{p}) - k_\mu (p + \bar{p})_\nu}{s} \right) \epsilon_\nu^* \mathcal{A}_\gamma(s), \quad (3)$$

$$\mathcal{M}_{\text{pole}}^Z = \frac{\alpha^2 m_W}{\sin^3\theta_W} \bar{v}(\bar{p})\gamma_\mu (v + \gamma_5) u(p) \left(\frac{\delta_{\mu\nu} k \cdot (p + \bar{p}) - k_\mu (p + \bar{p})_\nu}{(s - m_Z^2) + im_Z \Gamma_Z} \right) \epsilon_\nu^* \mathcal{A}_Z(s), \quad (4)$$

$$\begin{aligned} \mathcal{M}_{\text{box}}^Z = & -\frac{\alpha^2 m_Z}{4 \sin^3\theta_W \cos^3\theta_W} \bar{v}(\bar{p})\gamma_\mu (v + \gamma_5)^2 u(p) \{ [\delta_{\mu\nu} k \cdot p - k_\mu p_\nu] \mathcal{B}_Z(s, t, u) \\ & + [\delta_{\mu\nu} k \cdot \bar{p} - k_\mu \bar{p}_\nu] \mathcal{B}_Z(s, u, t) \} \epsilon_\nu^*, \end{aligned} \quad (5)$$

$$\begin{aligned} \mathcal{M}_{\text{box}}^W = & \frac{\alpha^2 m_W}{2 \sin^3\theta_W} \bar{v}(\bar{p})\gamma_\mu (1 + \gamma_5)^2 u(p) \{ [\delta_{\mu\nu} k \cdot p - k_\mu p_\nu] \mathcal{B}_W(s, t, u) \\ & + [\delta_{\mu\nu} k \cdot \bar{p} - k_\mu \bar{p}_\nu] \mathcal{B}_W(s, u, t) \} \epsilon_\nu^*, \end{aligned} \quad (6)$$

where $s = -(p + \bar{p})^2$, $t = -(p - k)^2$ and $u = -(\bar{p} - k)^2$. Here, v denotes the $\mu\bar{\mu}Z$ vector coupling constant, $v = 1 - 4 \sin^2\theta_W$. In terms of the scalar functions defined in the appendices of our previous paper [4], we have [6]

$$\begin{aligned} \mathcal{A}_\gamma(s) = & \left\{ 4 \left(6 + \frac{m_H^2}{m_W^2} \right) C_{23}(s, m_H^2, m_W^2) - 16 C_0(s, m_H^2, m_W^2) \right. \\ & \left. - \frac{16}{3} \frac{m_t^2}{m_W^2} \left(4 C_{23}(s, m_H^2, m_t^2) - C_0(s, m_H^2, m_t^2) \right) \right\}, \end{aligned} \quad (7)$$

$$\begin{aligned} \mathcal{A}_Z(s) = & \left\{ \left(5 - \tan^2\theta_W + \frac{m_H^2}{2m_W^2} (1 - \tan^2\theta_W) \right) C_{23}(s, m_H^2, m_W^2) \right. \\ & + (\tan^2\theta_W - 3) C_0(s, m_H^2, m_W^2) \\ & \left. - \frac{1}{2} \frac{m_t^2}{m_W^2} \frac{1 - (8/3) \sin^2\theta_W}{\cos^2\theta_W} \left(4 C_{23}(s, m_H^2, m_t^2) - C_0(s, m_H^2, m_t^2) \right) \right\}, \end{aligned} \quad (8)$$

$$\mathcal{B}_Z(s, t, u) = A(s, t, u), \quad (9)$$

$$\mathcal{B}_W(s, t, u) = A_1(s, t, u) + A_2(s, u, t), \quad (10)$$

with m_t denoting the top quark mass. In this case, it is the helicity flip contributions from the factors $\bar{v}(\bar{p})\gamma_\mu u(p)$ and $\bar{v}(\bar{p})\gamma_\mu\gamma_5 u(p)$ which survive in the $m_\mu \rightarrow 0$ limit. This can be seen by noting that, in the center of mass, we have

$$\bar{v}_+(\bar{p})\gamma_\nu u_+(p) = im_\mu(\bar{p} - p)_\nu / |\mathbf{p}|, \quad (11a)$$

$$\bar{v}_+(\bar{p})\gamma_\nu\gamma_5 u_+(p) = im_\mu(\bar{p} + p)_\nu / E, \quad (11b)$$

$$\bar{v}_+(\bar{p})\gamma_\nu u_-(p) = -2\sqrt{2}iE\xi_\nu^{(-)}, \quad (11c)$$

$$\bar{v}_+(\bar{p})\gamma_\nu\gamma_5 u_-(p) = -2\sqrt{2}i|\mathbf{p}|\xi_\nu^{(-)}, \quad (11d)$$

with $\xi_\nu^{(-)} = (1, -i, 0, 0)/\sqrt{2}$. If we define $\mathcal{M}^{\text{loop}}$ as

$$\mathcal{M}^{\text{loop}} = \mathcal{M}_{\text{pole}}^\gamma + \mathcal{M}_{\text{pole}}^Z + \mathcal{M}_{\text{box}}^Z + \mathcal{M}_{\text{box}}^W, \quad (12)$$

then $\mathcal{M}^{\text{loop}}$ is predominantly helicity flip.

IV. DISCUSSION

The differential cross section $d\sigma(\mu\bar{\mu} \rightarrow H\gamma)/d\Omega_\gamma$ is given by

$$\frac{d\sigma(\mu\bar{\mu} \rightarrow H\gamma)}{d\Omega_\gamma} = \frac{1}{256\pi^2} \frac{s - m_H^2}{\beta s^2} \sum_{\text{spin}} |\mathcal{M}^{\text{tree}} + \mathcal{M}^{\text{loop}}|^2, \quad (13)$$

with $\beta = \sqrt{1 - 4m_\mu^2/s}$. When integrating Eq.(13) to obtain the total cross section, we expect the contributions from the interference terms to be suppressed, since $\mathcal{M}_{\pm\mp}^{\text{tree}}$ and $\mathcal{M}_{\pm\pm}^{\text{loop}}$ both contain an additional factor of m_μ . This conclusion can only be invalid if the angular integration of the muon propagator factors $(1 \pm \beta \cos \theta)^{-1}$ in Eqs. (2) produce inverse powers of m_μ . This is not the case. For the $++$ or $--$ interference terms, the tree and loop amplitudes contain a factor of $\sin \theta$, which ensures that the angular integral is well behaved in the $\beta \rightarrow 1$ limit. The integral of $+ -$ and $- +$ interference terms can produce a factor of β^{-1} , but this, too, is finite as $\beta \rightarrow 1$. As a consequence, we can simply add the tree [7] and one-loop cross sections to obtain $\sigma(\mu\bar{\mu} \rightarrow H\gamma)$.

The result is illustrated in Fig. 3, where the tree, one-loop and total cross sections are plotted for several values of m_H as a function of the collider energy. For collider energies $\sqrt{s} \gtrsim 500$ GeV, the one-loop contribution exceeds the tree contribution. Note that Fig. 3 should not be taken literally at $\sqrt{s} \approx m_H$, where $\omega \rightarrow 0$ and the tree-level process is, in fact, the soft (infrared-divergent) QED correction to the resonance process $\mu\bar{\mu} \rightarrow H$. Here, we are concerned with production of the Higgs with an observable, relatively hard photon. In Fig. 4, the total cross section is shown as a function of m_H for several collider energies. At 500 GeV, luminosities of order 100 fb^{-1} are needed to probe this channel. To make this statement more precise, we investigated the principal background $\mu\bar{\mu} \rightarrow b\bar{b}\gamma$ by adapting the amplitudes for $e\bar{e} \rightarrow \mu\bar{\mu}\gamma$ [8]. In Table I, the background contributions are shown for several cuts on the $b\bar{b}$ invariant mass $m_{b\bar{b}}$. In addition to these invariant mass cuts, we require the transverse momenta of the b , \bar{b} and γ to be greater than 15 GeV, their rapidities y to be less than 2.5 and the separation ΔR between the γ and the b and the γ and the \bar{b} to be greater than 0.4. The background is compared to the signal in Table II for Higgs boson masses of 100 GeV and 200 GeV. This comparison shows that, while not a discovery mode for the Higgs boson, photon-Higgs associated production can be observed with signal to square root of background ratios (S/\sqrt{B}) greater than 2 when $m_H > 100$ GeV at a 500 GeV collider.

Finally, the presence of a large one-loop contribution makes it possible to use $\mu\bar{\mu} \rightarrow H\gamma$ as a probe of the Higgs-boson coupling to W 's, Z 's and top quarks. To determine the sensitivity of the $H\gamma$ cross section to changes in Standard Model couplings, we have varied the $t\bar{t}H$ coupling by a factor λ [9]. The result is shown in Fig. 5, where the characteristic feature is the minimum in the cross section at the Standard Model value $\lambda = 1$. For $\lambda > 1$, the cross section rises significantly. At a 500 GeV collider, observation of $H\gamma$ production with a cross section of order 1 fb would indicate some type of anomalous coupling.

ACKNOWLEDGMENTS

This research was supported in part by the U.S. Department of Energy under Contract No. DE-FG013-93ER40757 and in part by the National Science Foundation under Grant No. PHY-93-07980.

REFERENCES

- [1] R. B. Palmer, A. Sessler and A. Tollestrup, *Progress on the design of a high luminosity $\mu^+ \mu^-$ collider*, BNL-63245 (1996).
- [2] J. F. Gunion, *Muon Colliders: The Machine and The Physics*, UCD-97-17, hep-ph/9707379 (1997).
- [3] V. A. Litvin and F. F. Tikhonin, *Associated production of $H\gamma$ or HZ pairs at $\mu^+ \mu^-$ collisions*, hep-ph/9704417 (1997).
- [4] A. Abbasabadi, D. Bowser-Chao, D. A. Dicus and W. W. Repko, Phys. Rev. D **52**, 3919 (1995).
- [5] A. Djouadi, V. Driesen, W. Hollick and J. Rosiek, University of Karlsruhe preprint KA-TP-21-96, hep-ph/9609420.
- [6] Equations (7) and (8) contain an additional factor of 2 in the top quark contribution compared to Ref. [4].
- [7] The $+-$ (and $-+$) amplitudes contribute at most a few percent to the tree level cross section for $500 \text{ GeV} \leq \sqrt{s} \leq 4 \text{ TeV}$ and $60 \text{ GeV} \leq m_H \leq 300 \text{ GeV}$.
- [8] F. Berends *et al.*, Nucl. Phys. B **206**, 61 (1982); Z. Xu, D-H Zhang, and L. Chang, Nucl. Phys. B **291**, 392 (1987).
- [9] H. E. Haber, G. L. Kane and T. Sterling, Nuc. Phys. B **161**, 493 (1979).

TABLES

\sqrt{s}	$45 \text{ GeV} < m_{b\bar{b}} < \sqrt{s}$	$97.5 \text{ GeV} < m_{b\bar{b}} < 102.5 \text{ GeV}$	$197.5 \text{ GeV} < m_{b\bar{b}} < 202.5 \text{ GeV}$
500 GeV	11.1 fb	1.16×10^{-1} fb	8.20×10^{-2} fb
1000 GeV	3.80 fb	2.69×10^{-2} fb	1.58×10^{-2} fb
2000 GeV	1.21 fb	6.83×10^{-3} fb	3.65×10^{-3} fb
4000 GeV	0.37 fb	1.81×10^{-3} fb	9.04×10^{-4} fb

TABLE I. Cross sections for the background process $\mu\bar{\mu} \rightarrow \gamma b\bar{b}$ are given for several cuts on the $b\bar{b}$ invariant mass $m_{b\bar{b}}$. The last two columns are 5 GeV bins indicating, respectively, the background associated with a Higgs boson of mass 100 GeV or 200 GeV.

\sqrt{s}	$\sigma(m_H = 100 \text{ GeV})$	S/\sqrt{B}	$\sigma(m_H = 200 \text{ GeV})$	S/\sqrt{B}
500 GeV	6.78×10^{-2} fb	1.99	8.76×10^{-2} fb	3.06
1000 GeV	2.46×10^{-2} fb	1.50	3.87×10^{-2} fb	3.08
2000 GeV	8.76×10^{-3} fb	1.06	1.04×10^{-2} fb	1.72
4000 GeV	1.54×10^{-3} fb	0.36	2.17×10^{-3} fb	0.72

TABLE II. The cross sections for the associated production of 100 GeV and 200 GeV Higgs bosons are shown together with the ratio of the signal to the square root of the background (S/\sqrt{B}) for several $\mu\bar{\mu}$ collider energies. A luminosity of 100 fb^{-1} is assumed.

FIGURES

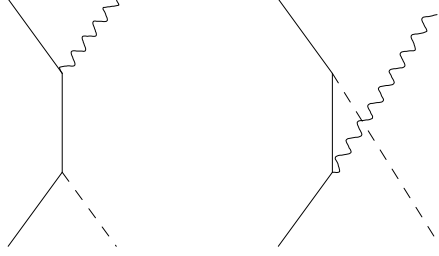


FIG. 1. Tree level diagrams for $\mu\bar{\mu} \rightarrow H\gamma$ are shown.

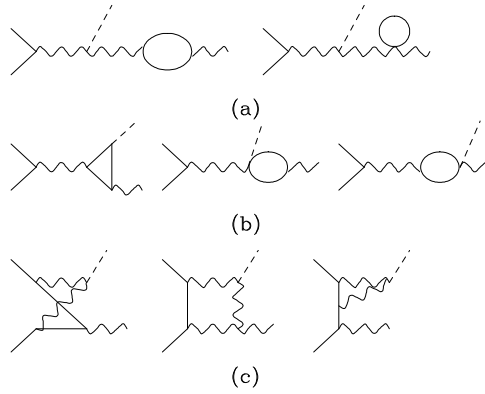


FIG. 2. Typical diagrams for the double pole (a), single pole (b) and box (c) corrections are shown. An external solid line represents a muon, a wavy line a gauge boson, a dashed line a Higgs boson and an internal solid line a muon, gauge boson, Goldstone boson or ghost.

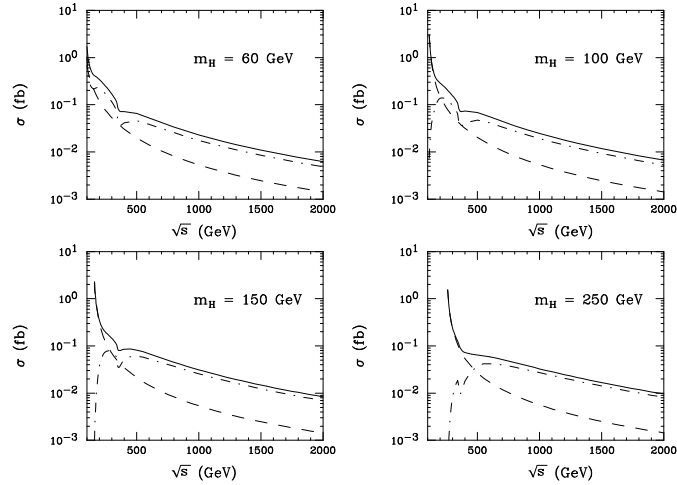


FIG. 3. The cross section for $\mu\bar{\mu} \rightarrow H\gamma$ resulting from the sum of the tree level and one-loop amplitudes is given for several values of m_H by the solid line. In each panel, the dashed line is the tree level contribution and the dot-dashed line is the one-loop contribution.

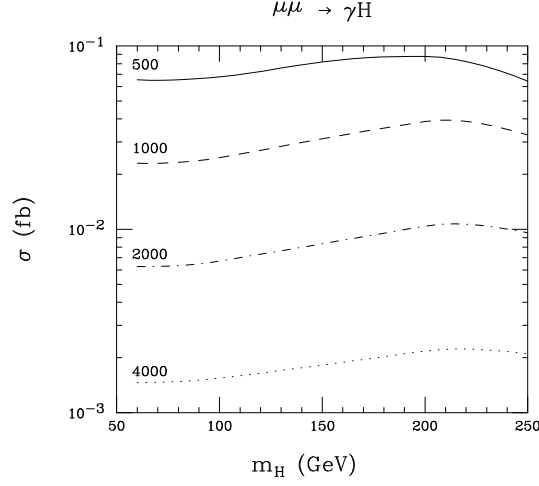


FIG. 4. The cross section for $\mu\bar{\mu} \rightarrow H\gamma$ resulting from the sum of the tree level and one-loop amplitudes is given as a function of m_H for collider energies of 500 GeV, 1000 GeV, 2000 GeV and 4000 GeV.

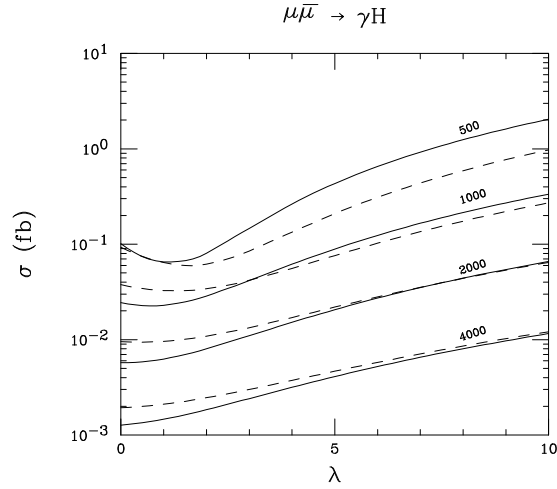


FIG. 5. The cross section for $\mu\bar{\mu} \rightarrow H\gamma$ obtained by scaling the Standard Model $t\bar{t}H$ coupling by a factor λ is shown for collider energies of 500 GeV, 1000 GeV, 2000 GeV and 4000 GeV. In each case, the solid line is $m_H = 60$ GeV and the dashed line is $m_H = 250$ GeV.